Secondary Control of Islanded Microgrids Using cascade PID Controllers tuned by combined GA and TLBO Algorithm

Reda Rabeh*'**‡, Mohammed Ferfra*, Ahmed Ezbakhe**

*Electrical Engineering department, Research Team in power and control (EREEC), Ecole Mohammadia d'Ingénieurs, Mohammed V University in Rabat, Morocco.

** Laboratory LERMA, ECINE, International University of Rabat, Sala Al Jadida, 11000, Morocco

(reda.rabeh93@gmail.com, ferfra@emi.ac.ma, ahmed.ezbakhe@uir.ac.ma)

‡ Corresponding Author; Reda Rabeh, Groupe Yasmine, Imm6, Apt 7, Mohammedia, Morocco, Tel: +212 697 244 699, reda.rabeh93@gmail.com

Received: 06.04.2023 Accepted:07.05.2023

Abstract- Nowadays, Microgrids are the more adopted in the electrification of autonomous aeras. The main idea of this study is managing frequency in an autonomous microgrid with renewable penetration. These microgrid systems aim to produce energy to reduce dependence on variable cost fuels and reduce harmful emissions into the atmosphere. The system under study is made up of a variety of energy sources, including controllable, renewable sources, as well as energy storage options. This combination is skillfully managed to ensure the MG's reliability and transparency in the face of intermittent power generation. Intermittent weather conditions from renewable sources and loads, such as temperature, solar radiation, wind speed, etc., indicate the numerous disturbances to the MG. Due to the active power compensation, these disturbances affect the power quality, especially the frequency. In order to solve this problem, it is highly recommended to intelligently manage the sources that can be controlled in order to reduce the frequency variation. This paper proposes a secondary frequency control with a cascade combination of three proportional integral and derivative (PID) as a reliable control technique under uncertainty. This controller is implemented in the input of the controllable sources in this study and tuned by a combined GA-TLBO as an efficient method to minimize the frequency fluctuation. An autonomous MG is simulated in MATLAB/Simulink and tested under numerous circumstances to validate the proposed method for generating the given parameters to reduce the frequency variation in various scenarios.

Keywords frequency control; autonomous microgrid; PID controller; Two cascade PID controllers; Three cascade PID controllers, GA-TLBO algorithm.

Nomenclature:

DE	: Differential evolution
DEG	: Diesel generator
DER	: Distributed energy resource
DG	: Distributed generator
EA	: Evolutionary algorithm
ESS	: Energy storage system
FC	: Fuel cell
GA	: Genetic algorithm
DE	: Differential Evolution
HS	: Harmony search
ISAE	: Integral Square Absolute Error
MG	: Microgrid
MOBHA	: Modified black hole optimization algorithm
MVO	: multi-verse optimization
MT	: Micro turbine
PI	: Proportional Integral

PID	: Proportional Integral and derivative
PSO	: Particle swarm optimization
PV	: Photovoltaic panel
TLBO	: Teaching Learning-Based Optimization
WOA	: Whale Optimization Algorithm
WT	: Wind turbine
FA	: Firefly Algorithm

1. Introduction

Microgrids have been the subject of several studies in various fields. In literature, several studies deal with the management of this systems because of the intermittence of their renewable sources and loads. For example, A. Goudarzi et all in [1] deal with the optimal economic power management of a reserve-constrained combined heat system based on a sequential hybridization of ETLBO and IPSO to beneficiate of performances of these two algorithms. In other case of study, authors of [2] present an economic and environmental study of a co-generation system based on the same approach in [1].

Moreover, at various levels of power generation, the output of renewable energy installations, such as photovoltaic and wind turbine panels, and energy storage systems is rising. One of the most well-known uses of these resources is in power systems called microgrids, which combine renewable energy sources with more traditional power plants like diesel engine generators to fulfill load demand. Combining these strategies attempts to cut down on reliance on fossil fuels, lower energy prices, and reduce harmful greenhouse gas emissions. By managing conventional sources and specialized resources like fuel cells, it offers flexibility, intelligence, and transparency while preventing frequency variation brought on by intermittent renewable sources and erratic load disturbance. The energy storage system may be used in the system as a source of generation in discharge mode or as a load in charge mode, and it is also used to increase the stability of the microgrid.

In the literature, several control techniques have been considered. In actuality, there are three basic levels of frequency control: primary control, secondary control, and tertiary control. The governor-turbine mechanism is used at the first level to manage the area frequency in order to handle modest deviations, but this is insufficient to swiftly restore the normal frequency in the presence of significant disruptions. Frequency control was a classic problem in different MG architecture. For example, in [3] authors develop a secondary frequency control in a conventional MR based on double Fed induction generator. Reference [4] highlights the role of IT for secondary control of a conventional power grid. With renewable penetration, authors of [5] present a study of a variable speed wind turbine with flywheel to maintain a dynamic stability of frequency in this MG. Using several controllers, secondary control is used in this situation to increase the stability of the microgrid [6-9]. The simplest way to get the desired results was to adjust the PI controller using empirical techniques like Ziegler Nickols, which was employed in various applications. Despite its ease of use, when the system is subjected to a significant disturbance, the PI controller produces undesired overrun. Thus, a variety of techniques are used, including evolutionary algorithms [10–18], to modify the settings of this controller. An implementation of the fuzzy logic frequency controller based on PSO in a microgrid is shown in Reference [14]. WOA is developed by the authors in [15] to fine-tune the obtained PID controller. In particular, MVO in [16], robust PI controllers with time delays, and evolutionary algorithms to reach the optimal values of the PI controller, such as TLBO in [17] and GA and FA in [18], have been suggested as solutions to this problem. The PI controller is the most basic controller with widespread industrial use and acceptable performance. In systems with significant disturbances and fluctuations, it is ineffective. As shown in [19–24], the fractional order PI can solve this issue as a solution to assure the adaptability of the microgrid under such circumstances. This controller was tested in a parallel control structure proposed in [19]. In fact, the tuning the fractional PID controller was applied using various strategies. For example, H. Wang, et all in [20] propose a multi-objective external optimization in the dynamic model of MG, and authors of [21] present a hybrid ALO-pattern search optimized fractional order controller for a load frequency control of a multiarea system incorporating distributed generation resources, gate-controlled series capacitor along with high-voltage direct current. Then refence [22] shows a novel concept of fuzzy adaptive fractional order-PID controller to control frequency of a microgrid constituted under renewable sources uncertainties. Authors of [24] present a meta-heuristic optimization strategy on frequency excursion mitigation in a multi-source islanded energy System with fractional PID controller.

To manage the load and power under uncertainties based on the linearized state of the MG, for example, Bervani proposes two robust control techniques H∞, μ-synthesis in [25] and shows that the -synthesis strategy is resilient. Other approaches were adopted in frequency control. For example, authors of [26] present the sliding mode control to improve the performance of load frequency control. Reference [27] show an adaptive control to deal with this problem.

In other applications, authors of [28] demonstrate the efficiency of their proposed approach in shipboard frequency control. In the same application, but with a DC Microgrids, Z.

Jin et all in [29] highlight a hierarchical strategy in MG control with storage system. A review of power sharing control and frequency control was detailed in [30]. It examines and categorizes several methods to power sharing control concepts. Finally, the authors of [31] offer an optimization approach for determining the ideal architecture for a data communication network in a power system with distributed frequency management.

This study is a continuation of my earlier work in [32-34], in which an intelligent tuning of PI controller in [32] and Fuzzy logic PI controller in [33-34] in the researched controller under parameter and power uncertainties was performed. This paper focuses on:

- novel technique of frequency control in a microgrid that employs a cascade combination of three PID controllers tuned using GA-TLBO algorithm. The idea is to beneficiate of a parallel combination of linear controller to obtain best performances than classical PID controller.
- Tuning the proposed controller parameters using a hybrid approach by combining two EAs (GA and TLBO). This approach was chosen to ensure the best convergence performance in the optimization of ISAE of frequency.
- This tuning is applied to assure the flexibility and transparency of the microgrid. The linearized system will be simulated under uncertainties in order to test the controller's efficiency.

The following sections arrange the work presented: Part 2 offers the mathematical model of the MG and the researched MG system controller. Section 3 explains the formulation problem and the recommended controller parameter. The algorithm used to adjust the suggested controller settings is presented in Section 4. Part 5 discusses the simulation findings. Lastly, Section 6 gives conclusions.

2. Modeling of the Studied MG

2.1. Dynamic Model of MG

In this paper, a hybrid power system is used, with two renewable sources acting as disturbances (PV grid and wind turbine), regulated sources such as diesel engine generators (DEG), fuel cells (FC), and micro-turbines (MT), and a battery storage system. The AC MG study is summarized in Fig.1 where the frequency depends on the power balance between generation and load as expressed in Eq. (1).

$$P_{Load} = P_{PV} + P_{WT} + P_{DEG} + P_{MT} + P_{FC} + P_{BES} \quad (1)$$

Where P_{PV} denotes PV output power, P_{WT} denotes WT output power, P_{DEG} denotes DEG output power, P_{FC} denotes FC output power, P_{MT} denotes MT output power, P_{BES} denotes BES output power, and PLoad denotes load power. P_{BES} is positive when discharging and negative when charging.

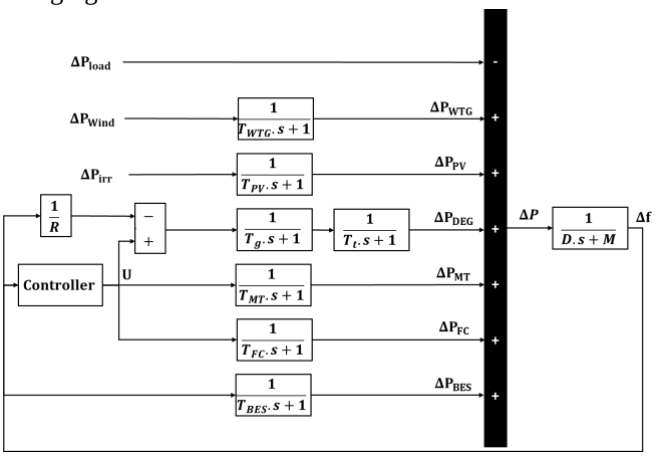

Fig 1. MG dynamical frequency response model

As previously described in the preceding paragraphs, PV, WT, and load are regarded as disturbances in the MG system to give frequency variation. Secondary frequency control, which is a combination of MT, DEG, and FC, is used to compensate for this erratic power. Each DER was represented by a basic, low-order linearized model in the investigated MG dynamic model to reflect the variations in DER output power. The following equation was devised to illustrate the changes in the MG DERs:

$$\Delta P_{Load} = \Delta P_{PV} + \Delta P_{WT} + \Delta P_{DEG} + \Delta P_{MT} + \Delta P_{FC} + \Delta P_{BES} \quad (2)$$

Equations for the MG dynamic frequency response model are provided in the following Eq (3-8), as seen in dynamic model. The two tables Table 1-2 indicate the MG parameters:

Table 1. MG rated power

Rated power (kW)		Rated power (kW)	
PV	5	BES	10
WT	5	DEG	20
FC	10	Load	60
MT	10		

Table 2. Parameters of the studied MG

Parameter	Value	Parameter	Value
D (pu/Hz)	0.015	T_{FC} (s)	4
M (pu)	0.1667	T_{MT} (s)	2
T_{PV} (s)	1,8	T_t (s)	0,4
T_{WT} (s)	1,5	T_g (s)	0,08
T_{BES} (s)	0,1	R (pu)	3

2.2. Renewable resources

Renewable resources are also known as uncontrolled sources due to their erratic nature and reliance on weather

conditions. The PV electric power and wind power output are generated by the solar radiation power and wind kinetic power, respectively. Equations (3-4) expresses the variation of output power PPV and PWT.

$$\Delta P_{PV} = \Delta P_{irr}.G_{PV} = \Delta P_{irr}.\frac{1}{1+T_{PV}.s} \quad (3)$$

$$\Delta P_{WT} = \Delta P_{wind}.G_{WT} = \Delta P_{wind}.\frac{1}{1+T_{WT}.s} \quad (4)$$

2.3. Controlled resources:

The Eq (5) defines the power change PMT. This DER tries to create electrical power from an input transforms hydraulic power. As shown in Eq (6), the energy conversion process for FC is defined as the use of chemical energy from the electrochemical reaction of hydrogen fuel and oxygen to generate direct current form of electricity. DG is a traditional controlled resource that combines an electrical motor and a governor (engine). The governor is in charge of controlling this DR, and Eq (7) can show how its power changes.

$$\Delta P_{MT} = U.G_{MT} = U.\frac{1}{1+T_{MT}.s} \quad (5)$$

$$\Delta P_{FC} = U.G_{FC} = U.\frac{1}{1+T_{FC}.s} \quad (6)$$

$$\Delta P_{DEG} = U.G_{DEG} = U\frac{1}{(1+T_t.s).(1+T_g.s)} \quad (7)$$

2.4. Energy Storage System:

This source's primary function is to supply load demand in discharging mode while storing excess production in charging mode. The goal is to maintain power balance in response to frequency fluctuations, as shown in Eq (8).

$$\Delta P_{BES} = \Delta f.G_{BES} = \Delta f.\frac{1}{1+T_{BES}.s} \quad (8)$$

The power fluctuation P and the dynamic model of are defined as follows:

$$\Delta P = \Delta P_{PV} + \Delta P_{WT} + \Delta P_{DEG} + \Delta P_{MT} + \Delta P_{FC} - \Delta P_{BES} - \Delta P_{Load} \quad (9)$$

$$\Delta f = \Delta P.G_{sys} = \Delta P\frac{1}{D+M.s} \quad (10)$$

3. Problem Formulation

A novel control method for secondary frequency control is developed in this paper. In several similar cases, the PI controller was used in these studies, which were tuned using a classical method such as the Ziegler Nichols method. The objective is to provide the best disturbance rejection possible. The frequency profile, on the other hand, appears to be inappropriate due to its large overshoot. To stay on track with this problem, other methods were used to compute the proposed controller parameters using GA-TLBO.

3.1. PID controller

Eq (11) and Figure 2 show the PID controller's equation law:

$$C_1(s) = K_p + \frac{K_i}{s} + K_d.s \quad (11)$$

The GA-TBLO algorithm is used to calculate Kp, Ki, and Kd as PID controller parameters. The purpose of this tuning is to reduce the IAE of frequency deviation as an objective function.

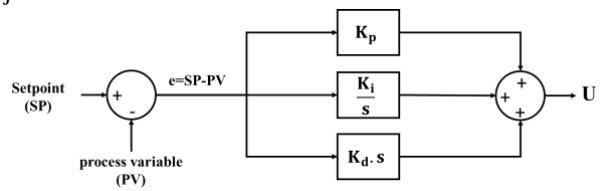

Fig 2. Block diagram of PID controller

3.2. Cascade Combination of two PID Controllers

In this control technics, we propose a cascade combination of two PID controllers. The investigated system to control power of FC, DEG, and MT to minimize frequency deviation under disturbance of renewable resources and load. It's depicted in Fig 3.

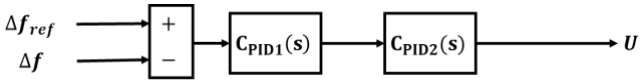

Fig 3. Block diagram of cascade combination of two PID controllers.

The general form of this controller law is expressed in Eq 12 as:

$$C_{2PID}(s) = C_{PID1}(s) * C_{PID2}(s)$$

$$C_{2PID}(s) = A_0 + \sum_{j=1}^{2}\frac{A_{-j}}{s^j} + \sum_{j=1}^{2} A_j.s^j \quad (12)$$

Where

$$A_0 = K_{p1} * K_{p2} + K_{i1} * K_{d2} + K_{i2} * K_{d1}$$

$$A_1 = K_{p2} * K_{d1} + K_{p1} * K_{d2}$$

$$A_2 = K_{d1} * K_{d2}$$

$$A_{-1} = K_{p2} * K_{i1} + K_{p1} * K_{i2}$$

$$A_{-2} = K_{i1} * K_{i2}$$

Where K_{p1} and K_{p2} are the proportional gain of the two controllers, K_{i1} and K_{i2} are the integral gain of the two controllers, K_{d1} and K_{d2} are the derivative gain of the two controllers.

3.3. Cascade Combination of Three PID Controllers

In this paper, a cascade combination of three PID controllers is used with the following controller law and Figure 4:

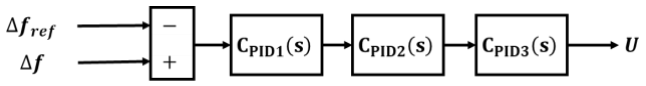

Fig 4. Block diagram of the proposed controller

The general form of this controller law is expressed in Eq (12) as:

$$C_{3PID}(s) = C_{PID1}(s) * C_{PID2}(s) * C_{PID3}(s)$$

$$C_{3PID}(s) = B_0 + \sum_{j=1}^{3} \frac{B_{-j}}{s^j} + \sum_{j=1}^{3} B_j . s^j \quad (13)$$

Where

$$B_0 = K_{p3} * A_0 + A_1 * K_{i3} + A_{-1} * K_{d3}$$

$$B_1 = A_0 * K_{d3} + A_1 * K_{p3} + A_2 * K_{i3}$$

$$B_2 = K_{p3} * A_2 + K_{d3} * A_1$$

$$B_3 = K_{d3} * A_2$$

$$B_{-1} = A_0 * K_{i3} + A_{-1} * K_{p3} + A_{-2} * K_{d3}$$

$$B_{-2} = K_{p3} * A_{-2} + K_{i3} * A_{-1}$$

$$B_{-3} = K_{i3} * A_{-2}$$

Where A_0 and K_{p3} are the proportional gains, A_{-1}, A_{-2} and K_{i3} are the integral gains, A_{-1}, A_{-2} and K_{i3} are the derivative gains.

3.4. The Importance of the Parallel Processing of PID Controllers

The parallel processing allows the creation of higher derivatives and integral orders in the controller law as shown in section 3. The importance of the parallel processing was briefly explained in the paper in section 5 as discussion of the results. For a classical PID controller, the integral term aims to eliminate the error in the input of controller and the derivative term improve the rapidity but affect the stability. The parallel processing creates an additional second derivative and integral order in the 2 parallel PID controller. A third derivative and integral order is added in the three parallel PID order.

The second and the third integral order reinforce the elimination of the error, but it affects the rapidity comparing to the classical integral controller. Moreover, the second and the third derivative order increase the rapidity, but it badly affects stability comparing to the integral controller. Then combing all these terms and tuning effect their gains will improve the performances of the two and three parallel PID controller in front of the classical PID controller. In section 5, a comparison between the three methods will be made to see and analyze the behavior of the three different controllers.

3.5. The Fitness Function.

The goal is to minimize the ISAE of frequency deviation as the objective function when tuning the controller parameters using the combined GA-TLBO Algorithms.

The variable decision for each controller is made up of its parameters. The variable decision for the PID controller is a vector of 3 elements expressed as $X_{PID} = [K_p\ K_I\ K_d]$. The variable decision with the cascade two PID controllers is composed of 6 scalar variables as $X_{2PID} = [K_{p1}\ K_{i1}\ K_{d1}\ K_{p2}\ K_{i2}\ K_{d2}]$. For the proposed controller with three PID cascade controllers, we define the variable decision, which is made up of 9 elements, as $X_{3PID} = [K_{p1}\ K_{i1}\ K_{d1}\ K_{p2}\ K_{i2}\ K_{d2}\ K_{p3}\ K_{i3}\ K_{d3}]$. The optimization is carried out with the primary goal of minimizing the ISTE while keeping the bounds of decision variables in mind. The mathematical model is illustrated in the following equations (14-15):

$$F_{Obj} = \int_0^T |\Delta f|^2 . dt \quad (14)$$

$$(X_{Jmin})_{J=1,n} \leq (X_J)_{J=1,n} \leq (X_{Jmax})_{J=1,n} \quad (15)$$

where X_J is the J^{st} element of the variable X, n is the variable decision size (3 for PID, 6 for two cascade PID controllers, and 9 for the proposed controller), and X_{Jmin} and X_{Jmax} are the lower and upper values of the variable X.

3.6. Evolutionary Algorithms Performances

The two main criteria for selecting the top EA are the global and local best search performances. The first one is the best objective function value, and by this criterion, the least number of iterations is the best. The variance of the population is used in Eq. (16) to get the second one. In reality, EA ceases to operate when the candidate solution remains unchanged, causing the fitness function to settle before the population variance.

$$S^2 = \frac{1}{N-1} . \sum_{i=1}^{N} (f_i - f) \quad (16)$$

Where N is the number of particles, f_i is the fitness values of the i^{st} individual and f is the mean of fitness values of population.

In the next sections 4 and 5, we will define the six EA adopted in this work and we will run and explore results to select the two best algorithms in the two criterions.

4. Optimization Algorithm

This paper presents some EA algorithms as genetic algorithm (GA), differential evolution (DE), harmony search (HS) and teaching learning-based optimization (TLBO).

4.1. Genetic Algorithm

The process of natural selection inspired the GA metaheuristic optimization. This method is defined by three operators: mutation, crossover, and selection, which are used to get the best potential solution.

- Mutation is the process of modifying an individual from a previous population in order to generate a greater rival (solution). It is distinguished by its poor probability of escaping the random search.
- Recombination or crossover attempts to develop a new candidate by combining the genetic composition of two parents.
- Selection is a function that assesses an individual based on the fitness function values.

It is achieved after the recombination process by choosing certain genomes from a population.

4.2. Particle Swarm Optimization Method

Kennedy and Eberhart developed the metaheuristic technique known as particle swarm optimization (PSO) in 1995 [15]. It enhances a candidate solution from a very large space of candidate solutions, starting with a randomly chosen population, to maximize a problem specified by an objective function. depending on particle movement modeled by the flocking behavior of birds, this method limits the search space depending on the position and velocity of the particles. The particle's path is dictated by its local best-known position in order to reach the best-known locations in the search space. This should focus the swarm's attention on the best choices. One definition of velocity is:

$$V_{k+1} = w.V_k + b_1.(P_i - X_k) + b_2.(P_g - X_k)$$

variable decision: $X_{k+1} = X_k + V_{k+1}$

where:

V_{k+1} is the updated velocity, V_k is the actual velocity, w is the inertia weight, b_1 is the global learning coefficient, P_i is the global best particle, X_k is the k^{tk} particle, b_2 is the personal learning coefficient and P_g is the local best solution.

4.3. Differential Evolution

DE is a stochastic, population-based optimization technique created by Storn and Price in 1996 to optimize real parameter, real valued functions. The population in this algorithm is made up of agents who migrate to the optimal place. It is made up of mutation, recombination, and selection [21]. These sections are repeated until a criterion is achieved.

Where:

-Mutation: this step consists on creating a new vector named donor vector Vf_{G+1} from previous ones named target vectors X_i using a mutation factor F:

$$\mathrm{Vf}_{G+1} = \mathrm{X}_1 + \mathrm{F}(\mathrm{X}_2 + \mathrm{X}_3)$$

-Recombination: It combines successful solutions from the previous generation to develop the trial from the target vectors and the donor vector from the previous step with a probability Cr.

-Selection: in this level, the target vector is compared with the trial vector and the one with the lowest function value is admitted to the next generation.

4.4. Teaching Learning-Based Optimization

The TLBO algorithm is motivated by a teacher's effect on the production of students in a class. It is organized into two primary phases: instructor and learner. The algorithm's goal is to turn all learners into instructors.

- The teacher phase is the period during which students get instruction from the instructor in order to achieve excellent marks. The caliber of the teacher and the other students in the class, on the other hand, has an impact on a student's grade. As a result, the top students are considered as instructors, while the remainder are simply students.
- Student phase: The interactions of a random student with other students serve as the foundation for their learning. At this phase, a student is randomly partnered with another student. If the second student obtains less information than the first, he will approach his colleague; else, he will withdraw.

This method is repeated until the halting requirements are met.

4.5. Biogeography-Based Optimization

The novel technique to problem solving, known as BBO [23], has several characteristics in common with earlier biology-based algorithms. A good solution corresponds to an island with a high HSI, whereas a poor solution denotes an island with a low HSI, according to the BBO hypothesis. Solutions with high HSI are more successful in preventing change than those with low HSI. BBO is the study of species extinction, speciation, and migration. The migration of a species from one island (habitat) to another, the emergence of new species, and the extinction of existing species are all described by mathematical models of BBO. The first example given of how a natural process might be expanded to address optimization issues is the BBO optimization algorithm.

4.6. Harmony Search

HS is a metaheuristic optimization method based on music [16]. The search process in optimization may be compared to the improvisation process of a jazz musician. The goal is to achieve the best or optimal by idealizing the qualitative improvisation process and therefore translating music's beauty and harmony into an optimization technique through the search for perfect harmony.

5. Simulation Results

The goal of this part is to use EA to tune the three investigated controllers. The three controllers are compared using the MATLAB/Simulink program, with a common

population size of 100 people and a maximum iteration of 100 iterations set.

Prior to optimizing the three controllers, a simulation was conducted without control under the three perturbations (radiation power, kinetic power of wind and load). Figure 5 depicts the frequency deviation of the examined MG with wind kinetic power perturbation at T1=5s, irradiation power perturbation at T2=15s, and load power perturbation at T3=25s. The perturbations are represented by 0.5 pu step variation.

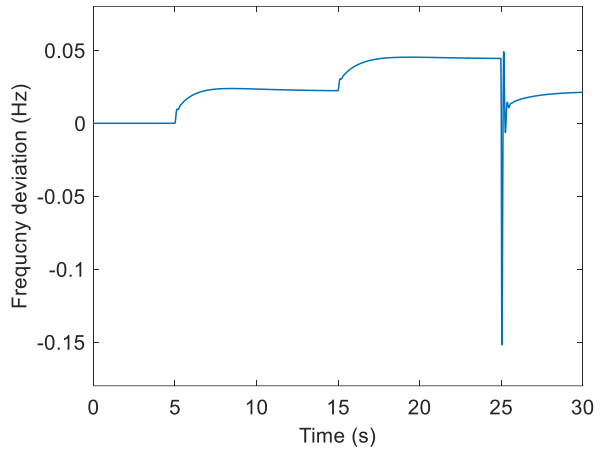

Fig 5. Frequency deviation without control

Fig 5 shows that the effect of load perturbation is the most significant when compared to irradiation and wind kinetic power (the fluctuation at T=25s). It is explained by the direct relationship between frequency deviation and load power deviation, as given in Eq (9-10). Nevertheless, the effect of the transfer function's step fluctuation in PV and WT power, as demonstrated in Eq (3-4). As a result, we will concentrate on the load perturbation in order to adjust the three controller parameters using the fours presented evolutionary algorithms in the previous sections (GA, DE, PSO and TLBO).

Table 3. Simulation results of fitness values with the fours controllers

Algorithm	Fitness function with PID	Fitness function with 2 cascaded PID	Fitness function with 3 cascaded PID
GA	$5.39 * 10^{-5}$	$9.89 * 10^{-6}$	$3.625 * 10^{-7}$
PSO	$5.408 * 10^{-5}$	$9.897 * 10^{-6}$	$3.633 * 10^{-7}$
DE	$5.392 * 10^{-5}$	$9.903 * 10^{-6}$	$3.618 * 10^{-7}$
TLBO	$5.4 * 10^{-5}$	$9.91 * 10^{-6}$	$3.63 * 10^{-7}$

Table 4. Simulation results of minimum of iterations with the fours controllers

Algorithm	Number of iterations with PID	Number of iterations with 2 cascaded PID	Number of iterations with 3 cascaded PID
GA	37	32	41
PSO	45	47	53
DE	53	62	84
TLBO	58	81	92

Table 5. Simulation results of variance values with the fours controllers

Algorithm	Variance value with PID	Variance value with 2 cascaded PID	Variance value with 3 cascaded PID
GA	$1.78 * 10^{-31}$	$2.51 * 10^{-34}$	$2.34 * 10^{-33}$
PSO	$1.77 * 10^{-33}$	$7.94 * 10^{-33}$	$1.26 * 10^{-36}$
DE	$2.37 * 10^{-36}$	$1.69 * 10^{-35}$	$1.41 * 10^{-41}$
TLBO	$1.45 * 10^{-39}$	$9.12 * 10^{-37}$	$4.17 * 10^{-42}$

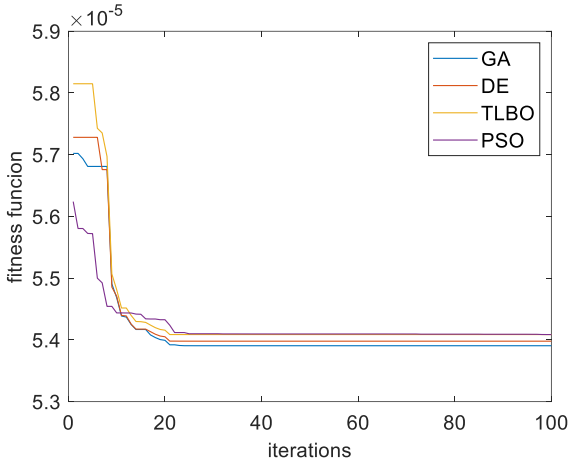

(a)

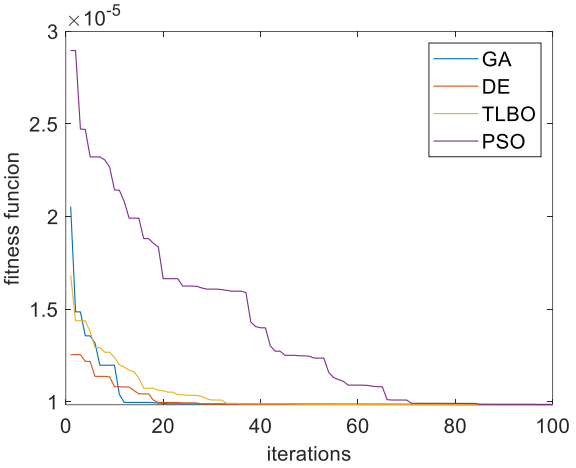

(b)

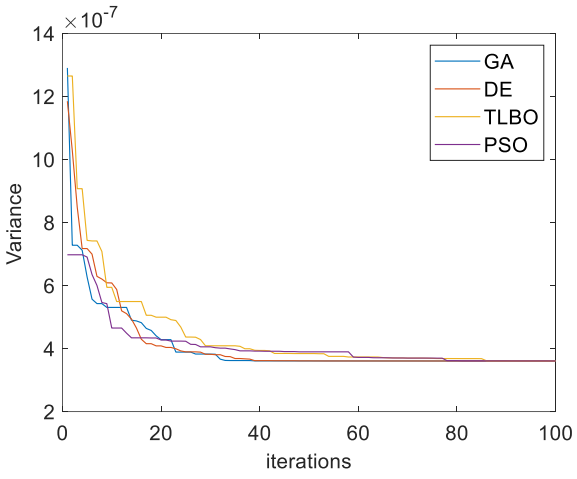

(c)

Fig 6. Fitness function variation of the four algorithms; (a) with PID controller; (b) with two cascaded PID controller; (c) with three cascaded PID controller

The simulations results are presented in the Tables 3-5 and Fig. 6. According to table 4 and Fig. 6, the GA provide the minimum iteration number of 37 in tuning PID controller comparing to DE and the two other EA. It has the best global convergence performance due to mutation. TLBO has the best local search property referring to Table 5. It shows the minimum variance value of $1.45 * 10^{-39}$ comparing to PSO and the two other EAs in tuning PID controller. They illustrate the global convergence property of GA and DE with their lower iteration number and TLBO and PSO demonstrate their local convergence with their minimum variance population value. Results confirm the same conclusions with two and three cascaded PID controllers. We propose to combine GA -TLBO as explained in the next part of this section.

5.1. Combined GA-TLBO Algorithm

We can select respectively GA an TLBO due to their best global and local convergence shown in the simulation results. The goal is to integrate both EA performances in order to benefit from them (as explained in the previous section). This novel technique combines GA's unpredictability with its higher overall performance and local convergence of TLBO, which is supported by population homogeneity and low variance values. The application of the recommended approach for decreasing frequency deviation is the main contribution of this study.

By alternating between the two approaches, the hybrid algorithm obtains the benefits of both GA and TLBO. In reality, GA produces a diversified population as a result of the algorithm's unpredictability, as well as an elite group that includes a few outliers. The TLBO algorithm will eliminate these worst solutions in order to safeguard the best individuals while improving the worst. Based on the variance of the population of solutions and the iteration value of each method, these two algorithms are alternated.

This strategy begins by producing the starting population at random while initializing the program settings (setting population size, decision variable boundaries, GA, and TLBO parameters). GA is the first algorithm to be employed due to the greater capabilities of global search. It is repeated until the population variance is less than the Set Variance Value, at which time TLBO is employed to eliminate any poor individuals created by GA. TLBO may take a long time and many iterations before meeting the stopping criteria while providing the greatest local search performance.

As a result, the variation in the best fitness function F Obj should be compared to a $\text{Set\_F}_{\text{Obj}}\text{\_Value} = 10^{-5}$. This contrast influences the decision to utilize GA or not. The combined GA-TLBO algorithm is depicted in the image below. $\text{Set\_Variance\_Value} = 10^{-5}$, $\text{Set\_F}_{\text{Obj}}\text{\_Value} = 10^{-5}$, $\text{Set\_Cpt1} = 5$ and $\text{Set Cpt2} = 5$ are the parameters chosen.

As shown in Fig. 7, the proposed technique begins by initializing the first population, F_{Obj}, to infinity and allowing index=0 in step 0. We initially assess the population's fitness value before deciding whether EA to run (GA or TLBO) and construct the next population. Next, we examine if index=0, F_{Obj}, and variance are less than their predetermined thresholds. If the maximum number of iterations is reached, the program stops; otherwise, the first step is repeated.

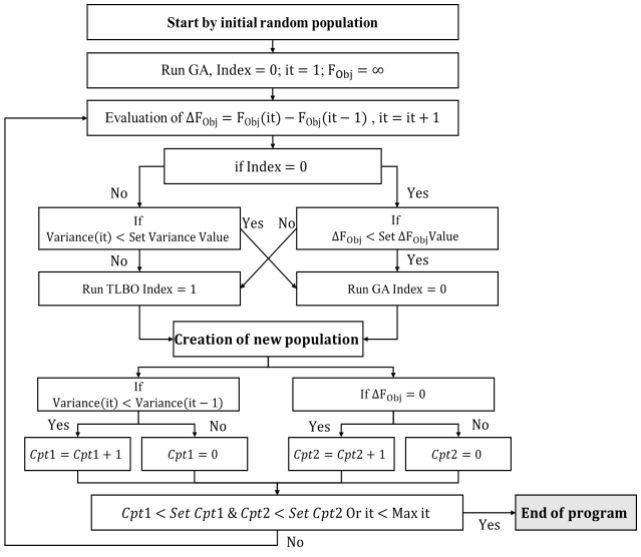

Fig 7. Flowchart of GA-TBLO algorithm

Using the combined GA-TLBO algorithm, the simulation results are shown in the tables 6-11 and Fig. 8. Figure 8 and Table 7 illustrate the effectiveness of the hybrid combination of GA-TBLO against GA and TLBO in the term of iteration number. Moreover, Table 8 confirms the best local search performance of the proposed method against GA and TLBO in PID. Numerical results are summarized in Table 6. Figure

11 depicts frequency deviation profiles. The optimization was carried out using a step change in load of 0.1 pu at T=1s. This is due to the most significant influence of load as the equivalent of total production.

Table 6. Simulation results of fitness values with the three controllers GA, TLBO and GA-TLBO.

Algorithm	Fitness function with PID	Fitness function with 2 cascaded PID	Fitness function with 3 cascaded PID
GA	$5.39 * 10^{-5}$	$9.89 * 10^{-6}$	$3.625 * 10^{-7}$
TLBO	$5.4 * 10^{-5}$	$9.91 * 10^{-6}$	$3.63 * 10^{-7}$
GA-TLBO	$5.392 * 10^{-5}$	$9.87 * 10^{-6}$	$3.61 * 10^{-7}$

Table 7. Simulation results of number of iterations with the three controllers GA, TLBO and GA-TLBO.

Algorithm	Number of iterations with PID	Number of iterations with 2 cascaded PID	Number of iterations with 3 cascaded PID
GA	37	32	41
TLBO	58	81	92
GA-TLBO	25	28	33

Table 8. Simulation results of variance values with the three controllers GA, TLBO and GA-TLBO.

Algorithm	Variance value with PID	Variance value with 2 cascaded PID	Variance value with 3 cascaded PID
GA	$1.78 * 10^{-31}$	$2.51 * 10^{-34}$	$2.34 * 10^{-33}$
TLBO	$1.45 * 10^{-39}$	$9.12 * 10^{-37}$	$4.17 * 10^{-42}$
GA-TLBO	$7.94 * 10^{-43}$	$2.51 * 10^{-45}$	$8.18 * 10^{-46}$

Table 9. PID controller tuned parameters with GA-TLBO.

K_p	K_i	K_d
373.6751	184.7626	122.8552

Table 10. Two cascade PID controllers tuned parameters with GA-TLBO.

K_{p1}	K_{i1}	K_{d1}	K_{p2}	K_{i2}	K_{d2}
90.855	39.248	9.366	89.176	16.802	6.195

Table 11. Proposed controller tuned parameters with GA-TLBO.

K_{p1}	86.198	K_{p2}	86.098	K_{p3}	71.3473
K_{i1}	2.254	K_{i2}	5.024	K_{i3}	6.334
K_{d1}	1.635	K_{d2}	1.745	K_{d3}	1.263

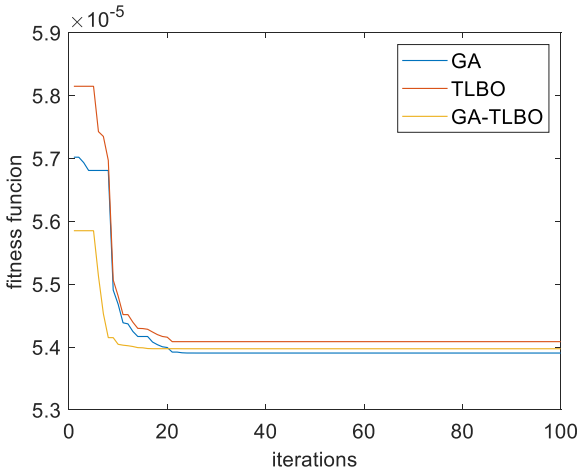

(a)

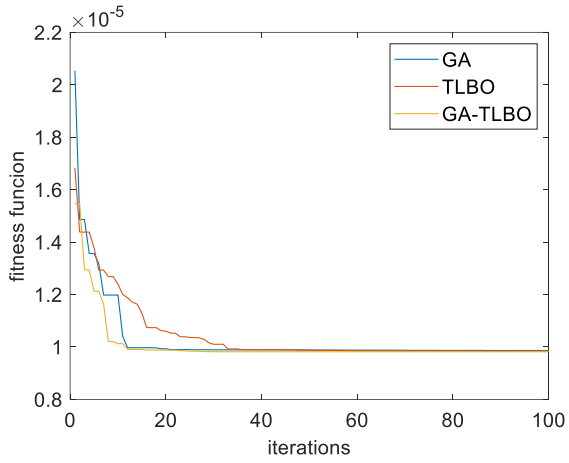

(b)

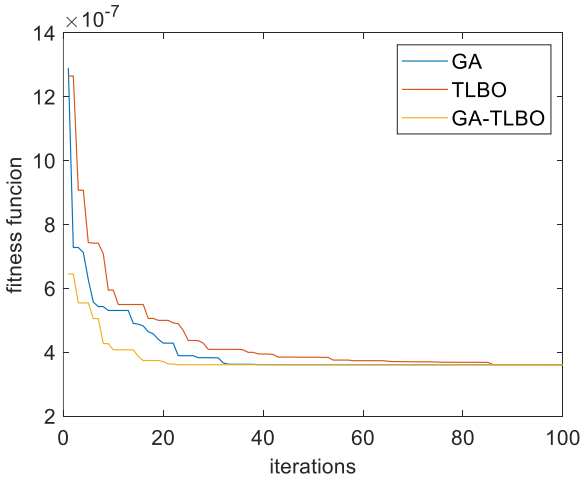

(c)

Fig 8. Fitness function variation of the three algorithms; (a) with PID controller; (b) with two cascaded PID controller; (c) with three cascaded PID controller

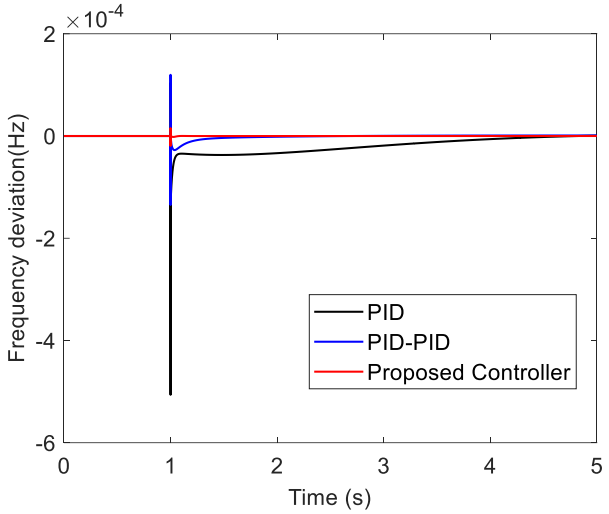

Fig 9. Frequency deviation with the three controllers using GA-TLBO algorithm.

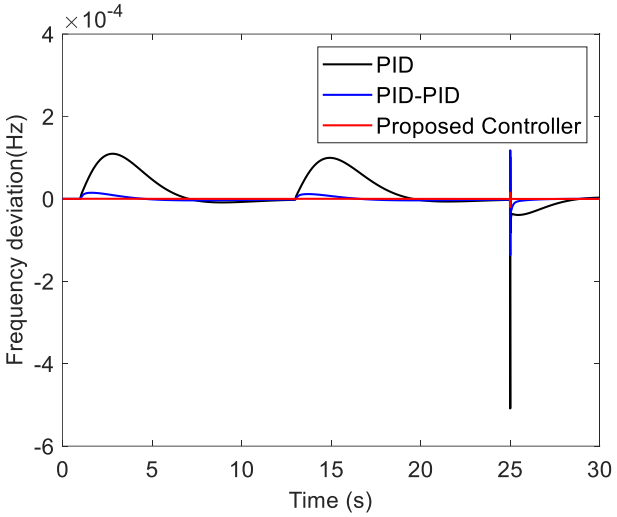

Fig 10. Frequency deviation using different controllers under different perturbations.

Table 6 shows that the suggested controller has the lowest fitness function value of $3.61 * 10^{-7}$ and the smallest frequency variation. The PID controller has the biggest overshoot against other controllers and with the higher rise time. The suggested solution provides the and excellent frequency deviation profile with lower overshoot and minimum rise time.

These results are explained by the second (and third) derivative and integral order respectively in PID-PID and the proposed controller in this paper. In fact, the integral terms aim to eliminate the error in the input of controller. This property is reinforced by the second and the third integral gains. The derivative gains anticipate the variation of error to rapidly seek the steady state value.

The combination of these higher derivative and integral orders improves the elimination of the overshoot and the rise time as illustrated in Fig 9. The red curve of the three PID controllers in cascade shows its performances against the PID-PID controller and PID controller.

To validate the three controllers adjusted in the preceding scenario, three distinct perturbations with three different step times are investigated. These perturbations are implemented as follows: at T1=1s, 0.5 pu is used to produce an irradiation power perturbation. A 0.5 pu kinetic power perturbation is injected at T2=13s, and a 0.1 pu perturbation is put under load at T3=25s.

In order to combine GA and TLBO, we establish two counters, Cpt1 and Cpt2, to calculate the number of consecutive GA or TLBO iterations. Set Cpt1 and Set Cp2 if Cpt1 and Cpt2 are less than their respective Set values. The frequency deviation profile obtained by the three tuned controllers is shown in Fig 10.

Table 12. Simulation results of different controllers under different perturbations.

Controller	Objective function
PID	$2.831 * 10^{-4}$
2 cascade PID controllers	$2.82 * 10^{-5}$
3 cascade PID controllers "Proposed controller"	$8.4 * 10^{-7}$

The suggested controller achieves the greatest results with the lowest frequency variation. Furthermore, according to Table 12, the ISTE of Δf with the cascade combination of three PID controllers is the lowest at $8.4 * 10^{-7}$. In comparison to PID and two PID controllers, the suggested controller achieves steady state faster than PID controller and PID-PID controller as illustrated in Fig 12.

5.2. Robustness of Proposed Method

A robustness study is performed to evaluate the resilience and efficacy of the proposed approach while taking into account the parameter uncertainties of the investigated system, as presented in Tab 13. The MG system program is run in this scenario with the various perturbations shown in the previous simulations. The goal is to see if the suggested controller maintains the same performance as the other two control techniques.

Table 13. Variation of MG parameters

Parameter	Value	Parameter	Value
D (pu/Hz)	+40%	T_{FC} (s)	15%
M (pu)	+40%	T_{MT} (s)	-10%
T_{PV} (s)	+20%	T_t (s)	25%
T_{WT} (s)	+25%	T_g (s)	-35%
T_{BES} (s)	+20%	R (pu)	-25%

Table 14 shows the values of the objective functions, and Fig. 11 shows the frequency deviation profiles of the three controllers.

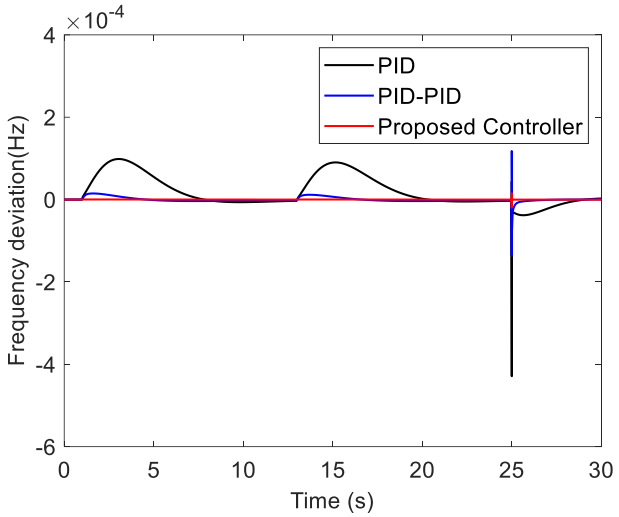

Fig 11. Frequency deviation with three controllers under uncertainty MG parameters.

Table 14. Simulation results of different controller under uncertainty MG parameters.

Controller	Objective function
PID	$2.7 * 10^{-4}$
2 cascade PID controllers	$2.82 * 10^{-5}$
3 cascade PID controllers "Proposed controller"	$8.4 * 10^{-7}$

The simulation results validate the robustness of the proposed controller. In fact, in Fig 13, this controller has the lowest fitness function and the smallest frequency deviation profile.

5.3. Simulation under Uncertainty

In this part, each DER power is affected by 10%. The goal is to test the efficacy of the proposed technique in the context of uncertain non-controllable source inputs. Under this ambiguous disturbance, it will have an effect on output power. As a result, power balance will become unstable, and frequency fluctuation will be greater than in previous circumstances. The simulation results are shown in Fig. 12 and Table 15.

Table 15. Simulation results under uncertainty

Controller	Objective function
PID	$2.831 * 10^{-4}$
2 cascade PID controllers	$4.957 * 10^{-5}$
3 cascade PID controllers "Proposed controller"	$8.493 * 10^{-7}$

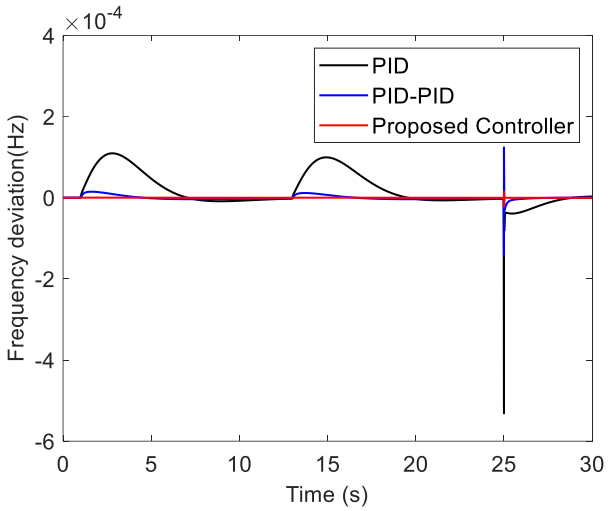

Fig 12. Frequency deviation using the three studied controllers under uncertainty of DG output power.

The suggested controller maintains its performance regarding the objective function and frequency variation. In addition, when compared to PID and two PID controllers, it maintains the optimal frequency deviation profile. The frequency deviation profile shows minimal overshoot and reaches steady state rapidly. Table 15 illustrates the efficiency of the adjusted prosed control with a lower minimal fitness function value than other controllers. These results show the proposed controller, as presented in this case of study.

5.4. Simulation under Variable Perturbation Profiles

In this subsection, the studied microgrid will be tested under variable perturbation profiles. The idea is to check the efficiency of the proposed controller under realistic irradiation, wind and load power profile. The following three figures presents respectively radiation and wind and a random load power profile.

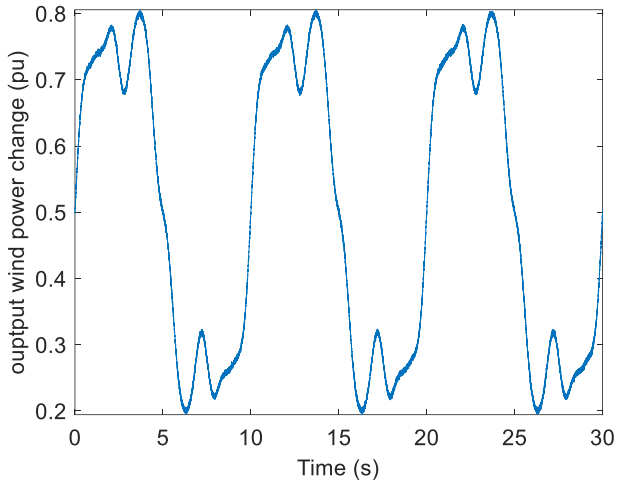

Fig 13. Wind turbine power variable changes.

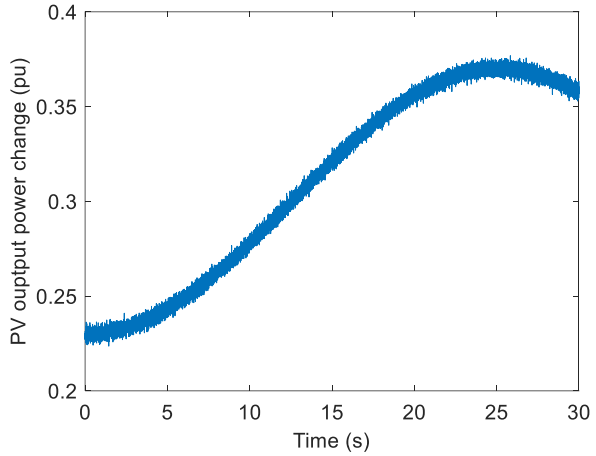

Fig 14. Irradiation power variable changes

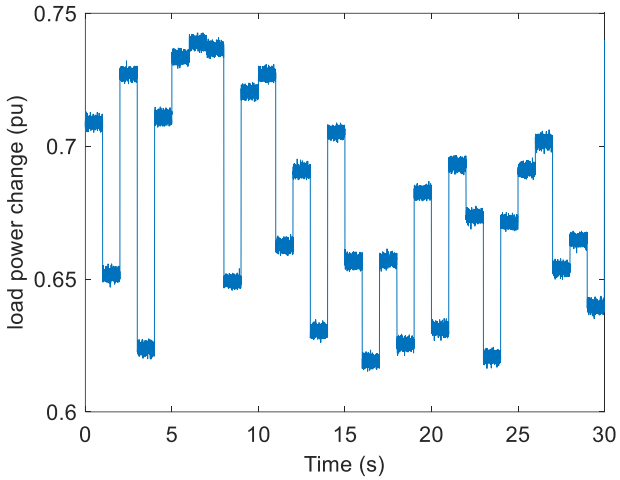

Fig 15. Load power variable changes

Table 16 displays the fitness function values for the three controllers investigated. These results support the suggested controllers' reliability and demonstrate the effectiveness of the cascade combination of three PID controllers as demonstrated in previous examples of research study.

Figures 16 and 17 depict the frequency deviations of the three controllers. It demonstrates the proposed controller's resilience in minimizing frequency deviation better than PID and cascade of two PID controllers, the most efficient classical algorithms discussed in this research study.

This is seen as a realistic circumstance that may have an impact on the MG. According to Fig 18, the deviation with the suggested technique is the best profile, which is very close to the required setpoint value of zero. As compared to PID and cascade of two PID controllers, it nearly always gives the least amount of variability. Table 16 summarizes all of the data that support the robustness of the suggested technique.

Table 16. Simulation results under variable perturbation profiles

Controller	Objective function
PID	$5.204 * 10^{-4}$
2 cascade PID controllers	$1.312 * 10^{-4}$
3 cascade PID controllers "Proposed controller"	$4.875 * 10^{-6}$

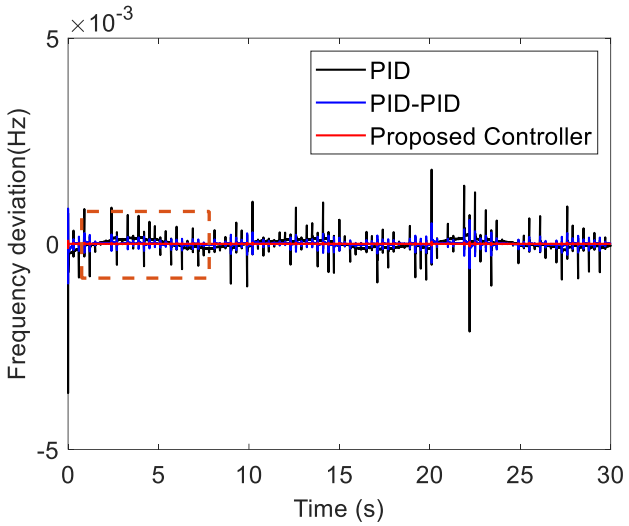

Fig 16. Frequency fluctuation under variable perturbation profiles

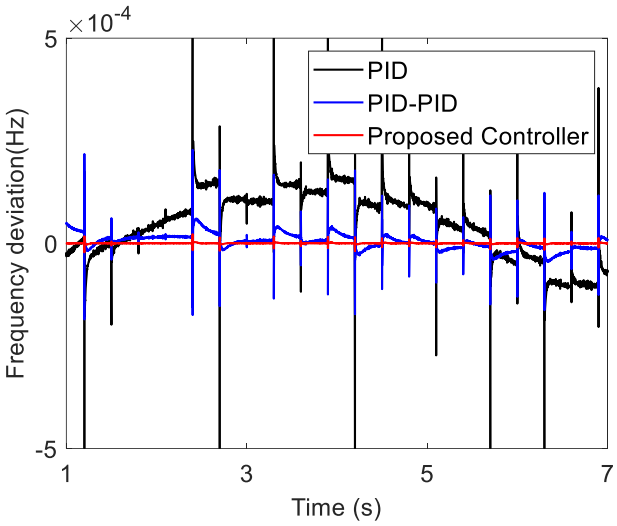

Fig 17. Frequency fluctuation under variable perturbation profiles between 1s and 7s

The proposed controller is used in this study for the secondary frequency control I, the examined MG. The combined GA and TLBO method is used to modify the settings of this suggested controller for efficiency. This controller was compared against PID and the cascade combination of two PID controllers, which were both adjusted using the same technique.

6. Conclusion

The investigated MG was created utilizing a linearized MG state-space model in which all DER are represented by a low order transfer function. The comparison of the three controllers emphasizes the accuracy of the suggested controller, which combines all of the performance of the two conventional controllers.

Results confirm the selection of GA and TLBO as algorithms which provide respectively the best global and local search performance. As said in section 5, with GA, the fitness function reaches its optimal value with the minimum of iteration number.

As compared to the cascade combination of two PID and three PID controllers, the single PID controller provides a high overshoot with a significant rising time and poor stability performance. The higher derivative order aims to reach the steady state value quickly than the derivative term of the PID controller. Also, the second and the third integral gain improve the elimination of the error comparing to the integral term of the PID controller. As a result, the suggested controller incorporates all of the performance demonstrated in the robustness research as well as varied perturbation profiles.

All of these results were evaluated in a robustness analysis using parametric uncertainties in microgrid parameters and uncertainties in DER power.

As implications of this work, we can investigate various control techniques, such as adaptive ones, to compare with the suggested method in this research, and examine additional system nonlinearities with greater complexity in the study. In a more modern MG system, it can additionally include predictions of the disturbances that are considered, such as kinetic and solar power.

References

[1] A. Goudarzi, S. Fahad, J. Ni, F. Ghayoor, P. Siano, and H. H. Alhelou, “A sequential hybridization of ETLBO and IPSO for solving reserve-constrained combined heat, power and economic dispatch problem”, Vol. 16, No. 10, pp. 1930-1949, May 2022, DOI: 10.1049/gtd2.12404.

[2] A. Goudarzi, C. Zhang, S. Fahad, A. J. Mahdi, “A hybrid sequential approach for solving environmentally constrained optimal scheduling in co-generation systems”, Energy Reports, Vol. 7, pp 3460–3479, 2017, DOI: 10.1016/j.egyr.2021.05.078.

[3] H. Benbouhenni, Z. Boudjema, and A. Belaidi, “A Direct Power Control of the Doubly Fed Induction Generator Based on the Three-Level NSVPWM Technique”, International Journal of Smart Grid, Vol. 3, No. 4, pp. 216-225, December 2019, DOI: 10.20508/ijsmartgrid.v3i4.

[4] Kenneth E. Okedu, “A Variable Speed Wind Turbine Flywheel Based Coordinated Control System for Enhancing Grid, Frequency Dynamics”, International Journal of Smart Grid, Vol. 2, No. 2, pp. 123-134, June 2018, DOI: 10.20508/ijsmartgrid.v2i2.

[5] Y. Andegelile, H. Maziku, N. Mvungi, and M. Kissaka, “Software Defined Communication Network Reliability for Secondary Distribution Power Grid”, International Journal of Smart Grid, Vol. 4, No. 3, pp. 117-124, September 2020, DOI: 10.20508/ijsmartgrid.v4i3.

[6] H. Bevrani, Robust power system frequency control. Power Electronics and Power Systems. Springer, 2nd ed, 2014, DOI: 10.1007/978-0-387-84878-5.

[7] I. Pan and S. Das, “Fractional order AGC for distributed energy resources using robust optimization”, IEEE Transactions on Smart Grid, vol. 7, no. 5, pp. 2175–2186, September 2016, DOI: 10.1109/TSG.2015.2459766.

[8] B. Yildirim, M. Gheisarnejad, M. H. Khooban, “A Robust Non-Integer Controller Design for Load Frequency Control in Modern Marine Power Grids”, IEEE Transactions on Emerging Topics in Computational Intelligence, Vol. 6, no 4, pp. 852 – 866, August 2022, DOI: 10.1109/TETCI.2021.3114735.

[9] Shubham, S. Prakash Roy, R. K. Mehta, and O.P. Roy, “Illustration of Load Frequency Control of Hybrid Renewable System With Tuned PIDF Controller”, 2021 Asian Conference on Innovation in Technology. DOI: 10.1109/ASIANCON51346.2021.9544649.

[10] M. F. Masood, M. I. Abid, Muhammad Shoaib Khalid, T. Murtaza, M. A. Rasheed, H. U. Rehman, and T. Zahid, “A Novel Solution to Eliminate Frequency Intermittency by Adding Spinning Reserve to the Micro-Hydro Turbine Generator Using Real-Time Control of Induction Motor through AC-DC-AC Power Converters”, International Journal of Smart Grid, Vol. 4, No. 4, pp. 149-156, December 2020, DOI: 10.20508/ijsmartgrid.v4i4.

[11] Y. Shan, J. Hu, K. W. Chan, Q. Fu, and J. M. Guerrero, “Model Predictive Control of Bidirectional DC–DC Converters and AC/DC Interlinking Converters—A New Control Method for PV-Wind-Battery Microgrids”, IEEE Transactions on Sustainable Energy, Vol. 10, No. 4, pp. 1823–1833, October 2019, DOI: 10.1109/TSTE.2018.2873390.

[12] T. Kerdphol, F. S. Rahman, M. Watanabe, and Y. Mitani, “Robust Virtual Inertia Control of a Low Inertia Microgrid Considering Frequency Measurement Effects”, IEEE Access, Vol 7, pp. 57550–57560, 26 April 2019, DOI: 10.1109/ACCESS.2019.2913042.

[13] I. Koley, A. Datta, G. K. Panda, S. Debbarma, “TLBO Optimised PIDD Controller for Coordinated Control in a Hybrid AC/DC Microgrid”, 2022 4th International Conference on Energy, Power and Environment (ICEPE). DOI: 10.1109/ICEPE55035.2022.9798062.

[14] R. R. Khaladkar, and S.N Chaphekar, “Particle swarm optimization-based PI controller for two area interconnected power system”, 2015 International Conference on Energy Systems and Applications, DOI: 10.1109/ICESA.2015.7503399.

[15] H.M. Hasanien,“Whale optimisation algorithm for

automatic generation control of interconnected modern power systems including renewable energy sources", IET Gen, Trans and Distr, Vol. 12, No. 3, pp. 607-614, February 2018, DOI: 10.1049/iet-gtd.2017.1005.

[16] D. Guha, P. K. Roy, S. Banerjee, "Multi-verse optimisation: a novel method for solution of load frequency control problem in power system", IET Gen, Trans and Distr., Vol. 11, No. 14, 3601-3611, 2017, DOI: 10.1049/iet-gtd.2017.0296.

[17] E.B. Elanchezhian, S. Subramanian and S. Ganesan, "Economic power dispatch with cubic cost models using teaching learning algorithm", IET Generation, Transmission & Distribution, Vol. 8, No. 7, July 2017, pp. 1187–1202, DOI: 10.1049/iet-gtd.2013.0603.

[18] A. V. Jha, D. K. Guptan and B. Appasani, "The PI Controllers and its optimal tuning for Load Frequency Control (LFC) of Hybrid Hydro-thermal Power Systems", 2019 International Conference on Communication and Electronics Systems, DOI: 10.1109/ICCES45898.2019.9002150.

[19] S. Kumar and M. N. Anwar, "Fractional order PID Controller design for Load Frequency Control in Parallel Control Structure", 2019 8th International Conference on Systems and Control (ICSC), 194-199, DOI: 10.1109/UPEC.2019.8893500.

[20] H. Wang, G. Zeng, Y. Dai, D. Bi, J. Sun, and X. Xie, "Design of a fractional order frequency PID controller for an islanded microgrid: A multi-objective extremal optimization method", Energies, vol 10, no 10, pp. 1502, DOI: 10.3390/en10101502.

[21] M. Raju, L. C. Saikia, and N. Sinha, "Load frequency control of a multiarea system incorporating distributed generation resources, gate-controlled series capacitor along with high-voltage direct current link using hybrid ALO-pattern search optimised fractional order controller", IET Renewable Power Generation, Vol. 13, Issue. 2, pp. 330–341 (2019), DOI: 10.1049/iet-rpg.2018.5010.

[22] D. Mishra, P. C. Sahu, R. C. Prusty and S. Panda, "A fuzzy adaptive fractional order-PID controller for frequency control of an islanded microgrid under stochastic wind/solar uncertainties", International Journal of Ambient Energy, Vol 43, No 1, pp. 4602-4611, 2022, DOI: 10.1080/01430750.2021.1914163.

[23] M. H. Khooban, T. Niknam, M. Shasadeghi, T. Dragicevic and F. Blaabjerg, "Load Frequency Control in Microgrids Based on a Stochastic Noninteger Controller", IEEE Transactions on Sustainable Energy, Vol. 9, No. 2, pp. 853–861, 2018, DOI: 10.1109/TSTE.2017.2763607.

[24] R. Venkatesh, P. Sharma; H. Siguerdidjane, D. Kumar and H. D. Mathur, "Frequency Excursion Mitigation in a Multi-source Islanded Energy System Using Meta-Heuristic Optimization Strategies" ,2020 IEEE 8th International Conference on Smart Energy Grid Engineering, DOI: 10.1109/SEGE49949.2020.9182006.

[25] H. Bevrani, M. R. Feizi and S. Ataee, "Robust Frequency Control in an Islanded Microgrid: H∞ and μ -Synthesis Approaches", IEEE Transactions on Smart Grid, Vol 7, No 2, March 2016, DOI: 10.1109/TSG.2015.2446984.

[26] G. Mahmoud, Y. Chen, L. Zhang, and M. Li, "Sliding Mode Based Nonlinear Load Frequency Control for Interconnected Coupling Power Network". Int. J. Control Autom. Syst., DOI: 10.1007/s12555-021-0678-8, 20, 3731–3739 (2022).

[27] M. Ghazzali, M. Haloua, and F. Giri, "Modeling and Adaptive Control and Power Sharing in Islanded AC Microgrids". Int. J. Control Autom. Syst., Vol. 18, pp. 1229–1241, 2020, DOI: 10.1007/s12555-019-0222-2.

[28] M. Khooban, T. Dragicevic, F. Blaabjerg, and M. Delimar. "Shipboard microgrids: A novel approach to load frequency control". IEEE Transactions on Sustainable Energy, Vol. 9, No. 2, pp. 843–852, 2018, DOI: 10.1109/TSTE.2017.2763605.

[29] Z. Jin, L. Meng, J. C. Vasquez, and J. M. Guerrero. "Frequency division power sharing and hierarchical control design for DC shipboard microgrids with hybrid energy storage systems". In 2017 IEEE Applied Power Electronics Conference and Exposition (APEC), pp. 3661–3668, 2017, DOI: 10.1109/APEC.2017.7931224.

[30] H. Han, X. Hou, J. Yang, J. Wu, M. Su, and J. M. Guerrero. "Review of power sharing control strategies for islanding operation of AC microgrids". IEEE Transactions on Smart Grid, Vol. 7, No. 1, pp. 200–215, 2016, DOI: 10.1109/TSG.2015.2434849.

[31] N. Gaeini, A. M. Amani, M. Jalili, and X. Yu. "Enhancing stability of cooperative secondary frequency control by link rewiring". In IECON 2017 - 43rd Annual Conference of the IEEE Industrial Electronics Society, pp. 5132–5137, 2017, DOI: 10.1109/IECON.2017.8216887.

[32] R. Rabeh, M. Ferfra, A. Ezbakhe, "Secondary Frequency Control of an Islanded Microgrid by Combined GA-TLBO Algorithm", 2019 8th International Conference on Systems and Control (ICSC), DOI: 10.1109/ICSC47195.2019.8950615, pp. 194-199.

[33] A Bouaddi, R Rabeh, M Ferfra, "MFO-WC Based Fuzzy logic PI Controller for Load Frequency Control of Autonomous Microgrid System", 2022 8th International Conference on Control, Decision and Information Technologies (CoDIT), DOI: 10.1109/CoDIT55151.2022.9803998, pp. 200-205.

[34] A Bouaddi, R Rabeh, M Ferfra, "Load Frequency Control of Autonomous Microgrid System Using Hybrid Fuzzy logic GWO-CS PI Controller", 2021 9th International Conference on Systems and Control (ICSC), DOI: 10.1109/ICSC50472.2021.9666683, pp. 554-559.